

submitted to The Astrophysical Journal, Letters

The First Deep ACS Ly α Images of Local Starburst Galaxies

Daniel Kunth

Institut d'Astrophysique, Paris, 98bis Bld Arago, F-75014, Paris, France

kunth@iap.fr

Claus Leitherer

Space Telescope Science Institute, 3700 San Martin Dr., Baltimore, MD 21218

leitherer@stsci.edu

J. Miguel Mas-Hesse¹

Centro de Astrobiología (CSIC-INTA), E-28850 Torrejón de Ardoz, Madrid, Spain

mm@laeff.esa.es

Göran Östlin

Stockholm Observatory, SE-106 91 Stockholm, Sweden

ostlin@astro.su.se

and

Artashes Petrosian

Byurakan Astrophysical Observatory and Isaac Newton Institute of Chile, Armenian Branch, Byurakan 378433, Armenia

artptrs@yahoo.com

ABSTRACT

¹Laboratorio de Astrofísica y Física Fundamental, POB 50727, E-28080 Madrid, Spain

We report the first results from a deep Ly α imaging program of local starburst galaxies with the Advanced Camera for Surveys (ACS) of the Hubble Space Telescope. The two observed galaxies ESO 350-IG038 and SBS 0335-052 have luminosities similar to those of the Magellanic Clouds but differ in their chemical composition. ESO 350-IG038 has an oxygen abundance of 1/8 solar, whereas SBS 0335-052 is known to have one of the lowest abundances among blue galaxies ($\sim 1/30$). The ACS imaging reveals a complex Ly α morphology, with sometimes strong offsets between the emission of Ly α and the location of stellar light, ionized gas traced by H α , and the neutral gas. Overall, more Ly α photons escape from the more metal- and dust-rich galaxy ESO 350-IG038. The absence of clear SBS 0335-052 Ly α emission over all observed knots, whatever their dust content or/and color indices, contradicts model expectations of a lower escape fraction from dust-rich gas due to destruction of Ly α photons by dust grains. Rather, the results are in qualitative agreement with models suggesting the kinematic properties of the gas as the dominant Ly α escape regulator. If the properties of the two observed galaxies are representative for starburst galaxies in general, Ly α will be difficult to interpret as a star-formation indicator, in particular if based on Ly α imaging at low spatial resolution.

Subject headings: galaxies: ISM — galaxies: starburst — galaxies: stellar content — ultraviolet: galaxies

1. Introduction

Ly α is now widely used as a tracer of galaxy formation and evolution in the high redshift universe. For several decades many observers have attempted to understand the conditions required to detect this line by focusing on nearby regions of rapid star formation. In a recent study, Kunth et al. (1998) discussed a set of eight nearby star-forming galaxies. They found four Ly α emitting galaxies with clear Ly α P-Cygni profiles indicating large-scale outflows of the interstellar medium (ISM). In contrast, the four remaining galaxies displayed damped Ly α absorption instead of emission, regardless of their dust content. Thuan & Izotov (1997) studied the unique starburst Tol1214-277 whose very strong and symmetric Ly α line shows no trace of blueshifted absorption.

The Space Telescope Imaging Spectrograph (STIS) on board HST was used to reobserve three of the galaxies discussed by Kunth et al. (1998): two with a Ly α P-Cygni profile and a third with only a broad Ly α absorption. 2-D analysis of these spectra clearly shows some partial decoupling of the UV continuum source and Ly α emission (Mas-Hesse et al.

2003). The spectra confirm the previous GHRS observations that favor a large Ly α escape probability when most of the neutral gas is velocity-shifted relative to the ionized regions and show that expanding shells of neutral gas can reach a few kpc wide.

These observational results are well reproduced by recent models of Tenorio-Tagle et al. (1999) for the evolution of a superbubble surrounding a starburst in a host galaxy. Whenever the neutral gas is outflowing, the Ly α photons redward of 1216 Å can escape. In contrast, no emission is detected if the ionized gas is shielded by a homogeneous slab of static neutral gas with column density above $N \approx 10^{18} \text{ cm}^{-2}$. On the other hand, diffuse Ly α may still be present and leaking out of the HI cloud, even if the HI is homogeneous and static. Finally, if the starburst is very young or if the HI coverage is static but porous, Ly α emission may be seen directly from the HII region, but with an intensity weaker than the recombination value. These results highlight the additional importance of the ISM properties for the escape probability of Ly α : The galaxies observed to date span a metallicity range of more than a factor of 10 but display no correlation between metal abundance and Ly α emission strength.

However additional parameters complicate the comparison between theory and observations: Ly α photons escape may critically depend on the column density and distribution of the neutral gas and dust, the morphology of the supershells, and probably on the luminosity of the burst and on the morphology of the host galaxy. In order to tackle these issues, a pilot Ly α *imaging* survey of nearby star-forming galaxies has been conducted using the Advanced Camera for Surveys (ACS) on board HST. An initial sample of six local starburst galaxies was chosen for Cycle 11, and here we report on initial results for the first two targets.

Throughout this paper we have assumed a value for the Hubble constant of $H_0 = 75 \text{ km s}^{-1}$

2. ACS observations and data reduction

30 orbits had been allocated to this program (GO-9470). Here we discuss the results for the first two galaxies ESO 350-IG038 and SBS 0335-052. Previous GHRS spectroscopy showed the first galaxy to be a Ly α emitter while the second exhibited a broad damped absorption. The observations were obtained with the Solar Blind Channel (SBC) of the ACS. Each galaxy was observed during five orbits in two adjacent filters. The F122M filter contains the Ly α emission, while the adjacent F140LP longpass does not transmit Ly α and was chosen for the continuum subtraction. The SBC uses a MAMA detector which is not subject to cosmic rays, and one single exposure per orbit was obtained in each filter. The F122M images were obtained during the “SHADOW” part of the orbit in order to lower

the background from geocoronal Ly α while the F140LP ones were acquired during the rest of the orbit. The total integration times per galaxy in the F122M and F140LP filters were 9095 and 2700 s, respectively. As a result of the larger bandwidth, the F140LP observations have approximately twice the S/N of the F122M data. The images were dithered using 3 positions with offsets of ~ 10 pixels in between. The SBC utilizes a pixel scale of $0.032''$, and the effective field of view is $31'' \times 35''$ (Pavlovsky et al. 2002).

The “drizzled” images produced by the standard pipeline for the two filters were combined after coalignment. From each combined image, the background was approximated by a surface (parameterized with a first-degree polynomial), and subtracted. Although weak in absolute terms in both filters, the background was significantly stronger in the F122M filter due to geocoronal emission. The images, calibrated in counts per second, were multiplied by the PHOTFLAM keyword from the image headers and converted to $\text{erg s}^{-1} \text{cm}^{-2} \text{\AA}^{-1}$ at the pivot wavelength of each filter (1274 and 1527 \AA , respectively).

Our ACS images were taken with the goal of detecting Ly α emission from massive star-forming regions, and possible diffuse emission. In order to detect the excess emission within the F122M filter that would be produced by the Ly α photons, we need to completely remove the continuum contribution. The subtraction procedure depends on the slope of the continuum, which might be variable for different regions over the images. Therefore, different normalizations between both filters were required for different regions.

We express the continuum spectral energy distribution as a power law: $f_\lambda \propto \lambda^\beta$. For a flat continuum ($\beta = 0$), the scaling factor between F122M and F140LP is 10.3, i.e., the ratio of the PHOTFLAM keywords. A redder SED with $\beta = 1$ gives a scaling factor of 12.5, and a bluer SED with $\beta = -2$ gives 7.2. We have used available spectroscopic UV data from GHRS (Thuan & Izotov 1997, Kunth et al. 1998) and IUE, as well as the optical to UV colors from HST photometry to estimate β and aid us in the continuum subtraction.

We stress that the continuum subtraction procedure is affected by several parameters, most importantly the intrinsic continuum slope of the stellar population. Moreover, a Ly α P-Cygni profile as frequently observed in these objects tends to hide the Ly α emission when imaged through this filter (the emission and the absorption wings tend to cancel, at least partially). Therefore, our results should be regarded qualitatively only.

Our subtraction technique is supported by the comparison with previous GHRS data. As discussed below, we find excess emission within the F122M filter where GHRS shows a prominent Ly α emission line as well (ESO350-IG038), while we detect a relative deficit of photons around Ly α where a strong and broad absorption profile is present (SBS0335-052).

3. Results and discussion

3.1. ESO350-IG038 (Haro 11)

This galaxy has a radial velocity of 6175 km s^{-1} and a complex morphology. The optical and near-infrared (IR) properties have been discussed by Vader et al. (1993), Heisler & Vader (1994), Bergvall et al. (2000), and Bergvall & Östlin (2002). The nebular oxygen abundance is $12+\log(\text{O}/\text{H})=7.9$ (Bergvall & Östlin 2002). Three bright condensations have been identified, all with strong $\text{H}\alpha$ emission. Following the nomenclature by Vader et al. (1993), we denote these by A, B, and C (see Fig. 1). Knot A has the bluest optical and near-IR colors and small reddening, $E(B - V) = 0.16$, as derived from $\text{H}\alpha/\text{H}\beta$. In contrast, B and C have redder colors and larger internal extinction, $E(B - V) \approx 0.4$. The galaxy has been imaged in the WFPC2/F606W filter in an HST snapshot program (Malkan et al. 1998) which has revealed numerous compact star clusters (Östlin 2000). A $\text{Ly}\alpha$ line exhibiting a P-Cygni profile was detected with HST/GHRS (Kunth et al. 1998).

Fig. 1 shows the F140LP, F122M, and continuum subtracted $\text{Ly}\alpha$ images. A relative scaling of 10.3 between F122M and F140LP was used, equivalent to $\beta = 0$. In Fig. 2 we show an RGB composite of optical, F140LP, and continuum subtracted $\text{Ly}\alpha$ images.

Figures 1 and 2 show that knot A is resolved into several bright star clusters, whereas B is more diffuse and C is dominated by a single luminous source. Comparison of the F140LP and F606W images shows the regions around A and C to have very blue UV/optical colors: $f_{\lambda, \text{F140LP}}/f_{\lambda, \text{F606W}} \approx 15$, implying $\beta = -2$, whereas in region B the average ratio is only 3, implying $\beta = -0.8$. The region east of C is redder, $f_{\lambda, \text{F140LP}}/f_{\lambda, \text{F606W}} \approx 1$, as seen also from Fig. 2.

$\text{Ly}\alpha$ emission is detected from region C. It is more extended along the north-south direction than the continuum, indicating that the emission is not isotropic. $\text{Ly}\alpha$ is detected in region A as well. Faint $\text{Ly}\alpha$ emission is seen over a large fraction of the galaxy, with the exception of region B and its immediate surroundings showing clear absorption. The emission in regions A and C has absorption cores near the knots. However, the absorption cores are shifted slightly to the north with respect to the emission. We have confirmed that this is not due to a misalignment of the F122M and F140LP images. After integration, the emission outweighs the absorption. A faint $\text{Ly}\alpha$ blob (labeled ‘D’ in Fig. 1), undetected in the continuum, is seen south-east of C.

The results are sensitive to the scaling of the two filters F122M and F140LP when subtracting the continuum. If we use the $f_{\lambda, \text{F140LP}}/f_{\lambda, \text{F606W}}$ ratio and assume a power law spectral energy distribution (SED) we obtain $\beta = -2$ to 0. Using this method to compute

a spatially varying scaling factor between F122M and F140LP, the effect is that only C and D shows significant emission. However, the GHRS spectrum of Kunth et al. (1998) shows a continuum decrease from 1300 to 1200 Å, indicating that one power law SED is not a good approximation over the full spectral range. Adopting the GHRS slope still leads to absorption from region B. Using the slope derived from an IUE spectrum ($\beta = -1$) gives a result similar to that presented in Fig 1; the emission close to A becomes weaker, but the diffuse emission remains. This illustrates the importance of determining the right continuum level. However, given the appearance of the continuum near Ly α from the GHRS spectra, it is clear that photometry always faces a potential risk of over- or underestimate the Ly α line strength.

The absorption in region B, and in the cores of the sources in A and C is too strong to be explainable by anything but a deep Ly α trough. Note that B still has rather blue UV to optical colors, so the absorption cannot be a spurious effect of reddening or an underlying red stellar population.

Double velocity components in H α with a velocity difference of $\sim 50 \text{ km s}^{-1}$ are seen in regions A, C, as well as B (Östlin et al. 1999). Kunth et al. (1998) detected broad metallic absorption lines from neutral gas blue-shifted by 60 km s^{-1} with respect to Ly α . At variance with SBS0335-052, no HI emission gas has been detected at a limit of $10^8 M_\odot$ (Bergvall et al. 2000), although Kunth et al. (1998) detected dense neutral gas in absorption. Hence the neutral gas distribution is likely to be clumpy, and any diffuse gas would be ionized, explaining why we detect Ly α in emission.

The small but systematic offset of Ly α to the south with respect to the continuum in regions A and C might be an indication of a velocity gradient in the neutral gas. This is consistent with the H α velocity field showing a global velocity gradient of the order of $10 - 15 \text{ km s}^{-1}$ per arcsec, or $25 - 40 \text{ km s}^{-1} \text{ kpc}^{-1}$ (uncorrected for inclination) with a kinematical major axis in the south-eastern direction, causing a blueshift of the gas to the south of A and C with respect to these regions (Östlin et al. 1999). The redshifted regions to the north of A and C do not show Ly α but these photons may be absorbed by the same gas complex responsible for the absorption in the center (region B). As discussed in detail in Mas-Hesse et al. (2003), the visibility of the Ly α emission increases with the blueshift of the neutral gas. While we expect Ly α photons to be escaping from the regions where the neutral gas is blueshifted, we do not expect emission in the absence of a velocity offset between the neutral and ionized regions. The absence of emission from region B might therefore indicate static neutral gas along our sight line. This galaxy illustrates the importance of the kinematic structure of the region for the emission of Ly α photons. The resulting Ly α distribution will be non-isotropic and much more complex than the H α distribution.

As mentioned above, the Ly α emitting regions show absorption cores. We attribute this effect to the known P-Cygni properties of the Ly α profiles in this galaxy: the stronger the stellar continuum, the deeper will be the blueshifted absorption wing (see Mas-Hesse et al. 2003 for details). Therefore, the emission wing tends to cancel with the absorption where the continuum is higher.

3.2. SBS0335-052

SBS0335-052 has a nebular oxygen abundance ($12 + \log(\text{O}/\text{H}) = 7.3$; Melnick et al. 1992). This value is almost as low as that of IZw18, triggering discussions whether SBS0335-052 is a truly young galaxy in its first burst of star formation (Thuan et al. 1997, cf. Östlin & Kunth 2001). The broad damped Ly α absorption reported by Thuan et al. (1997) from their GHRs spectra suggests a static HI reservoir surrounding the massive star condensations. The HI column density within the GHRs aperture amounts to $7.0 \times 10^{21} \text{ cm}^{-2}$. According to Mas-Hesse et al. (2003), the very young starburst episode would be starting to ionize the surrounding medium, but the mechanical energy released would still be insufficient to accelerate the large amount of HI gas in front of the region. The fits presented by these authors indicate that the intrinsic Ly α emission line could be very strong, with an equivalent width around 120 Å, as predicted by theoretical models. HST WFPC2 V and I images (Thuan, Izotov, & Lipovetsky 1997), UBVRI surface photometry by Papaderos et al. (1998), and near- and mid-IR imaging (Vanzi et al. 2000; Dale et al. 2001) have revealed several super star clusters (SSC). A comparison of the data of Thuan et al. with our ACS frames (Figs. 1 and 2) shows that the brightest star-forming knots in the visible and IR range (SSC1 and SSC2 in the notation of Thuan et al.) are not the brightest in the UV continuum. In contrast, SSC4 and SSC5 are much brighter in the UV than the other SSCs: $f_{\lambda, F140LP}/f_{\lambda, F791W} \approx 100, 100,$ and 35 for SSC4, SSC5, and SSC1, respectively. Our ACS images show that SSC3 is a well defined double system which is not resolved in the optical and near-IR.

A clear lack of photons within the Ly α filter is evident for the different SSCs on the image. This lack of photons is intrinsic, and is not related to any normalization effect. This is remarkable in view of the strong H α observed in this galaxy (e.g. Melnick et al. 1992) and the $f_{\lambda, F140LP}/f_{\lambda, F791W}$ colors. This absence is found both when the intrinsic slope of the UV continuum is used ($\beta = -2.5$) and also when a flat continuum ($\beta = 0$) is assumed. If β is estimated from $f_{\lambda, F140LP}/f_{\lambda, F791W}$, it is found to vary between -3 and -1.8 over the starburst region. Nevertheless, a weak and extended diffuse Ly α emission is detected around SSC5 to the N-E, as shown in Fig. 1 (bottom right). This emission is very weak, and its reality is

subject to the uncertainties in the continuum subtraction. Ly α photons could escape if they find a way: either through holes with lower HI column density, or regions where the neutral gas could be moving at some velocity with respect to the central HII region. Tenorio-Tagle et al. (1999) (see also Mas-Hesse et al. 2003) suggest that an ionized cone could develop through the surrounding neutral gas halo shortly after the ignition of a massive starburst. This cone would be oriented along the minor axis of the system. In this case, most of the gas towards the N-E of SSC5 could be already ionized, allowing some Ly α photons to escape. Thuan & Izotov (1997) found evidence for neutral gas flows, identifying two systems at -500 and -1500 km s $^{-1}$ with respect to the galaxy redshift. As concluded for ESO 350-IG038, the kinematic structure of the neutral gas in these regions could favor the escape of some Ly α photons in specific areas. Long-slit high-resolution spectroscopy would be needed to identify the dominant mechanism leading to the detection of Ly α photons.

In any case, the absence of clear net Ly α emission from all observed knots confirms what has already been discussed (Thuan et al. 1997; Kunth et al. 1998), supporting again the lack of correlation between Ly α fluxes and metallicities (hence dust) found by Giavalisco et al. (1996). The large aperture of the IUE satellite limited Giavalisco et al. to size scales of order kpc. Our highly resolved ACS images allow us to push the 1-pixel resolution down to 5.7 and 8.9 pc for ESO350-38 and SBS0335-052, respectively. If dust affects the Ly α escape, it must do so at even smaller spatial scales. While some dust is clearly present in SBS0335-052, SSC1 does not suffer from severe extinction (Thuan et al. 1997), and the same must be true for SSCs 4 and 5 in view of their UV to optical colors. Even if the emission close to SSC5 is real, it is very weak and completely negligible on the whole. The HI cloud around SBS0335-052 is clearly very dense and apparently static (at least in front of the SSCs), hence favoring the multiple scattering mechanism responsible for the attenuation.

4. Conclusions and implications for high-redshift galaxies

Our first ACS images of two dwarf starburst galaxies give us a view at the Ly α emission that is complementary to that of spectroscopy. These images already confirm the existence of two markedly different types of starburst galaxies: some are Ly α emitters, while others show rather broad absorption profiles. Even galaxies displaying Ly α emission may do so in a complex pattern, as we have shown in ESO350-38: two bright H α regions show emission, while a third one shows strong absorption. At high redshift, this morphological resolution is not attainable.

In many respects, Ly α could be a fundamental probe of the young universe. It suffers from fewer luminosity biases than Lyman-break techniques so that Ly α surveys become a

more efficient way to trace the fainter end of the luminosity function, i.e., it traces the building blocks of present-day galaxies in the hierarchical galaxy formation paradigm (Hu, Cowie, & McMahon 1998; Fynbo et al. 2001). Early results paint a complex picture. The equivalent widths of the sources are much larger than expected for ordinary stellar populations (Malhotra & Rhoads 2002). They could be explained by postulating an initial mass function (IMF) biased towards more massive stars, as predicted theoretically for a very metal-poor stellar population (Bromm, Coppi, & Larson 2001). The combined effect of low metallicity and flat IMF, however, can only partly explain the anomalous equivalent widths. Additional mechanisms must be at work. Could spatial offsets between the escaping Ly α and the stellar light, together with higher extinction of the dust shrouded stars be important? Our ACS imagery cautions against using the Ly α equivalent width as a star-formation indicator in the absence of spatial information.

The source numbers themselves are only about 10% of the numbers expected from an extrapolation of the Lyman-break luminosity function. Malhotra & Rhoads (2002) speculate if the youngest galaxies are preferentially selected, whereas older populations are excluded, the results are skewed towards large Ly α equivalent widths. Could dust formation after 10^7 yr destroy the Ly α photons? The results in the low-redshift universe suggests otherwise. We find no support for dust playing a *major* role in destroying Ly α photons. Rather, the ACS images favor the highly irregular gas morphology as key to understanding the Ly α escape mechanism via kinematic effects.

Haiman & Spaans (1999) proposed Ly α galaxies as a direct and robust test of the reionization epoch. Prior to reionization, these galaxies are hidden by scattering of the neutral intergalactic medium (IGM). Therefore, a pronounced decrease in the number counts of *galaxies* should occur at the reionization redshift, independent of Gunn-Peterson trough observations using *quasars*. Ly α in galaxies would have the additional appeal of being sensitive at much higher IGM optical depths since its red *wing* coincides with the red damping wing of intergalactic Ly α only. While this idea is attractive in principle, our ACS imagery calls for caution. In practice, Ly α is a complex superposition of emission and absorption in the star-forming galaxy itself. The resulting Ly α profile will be strongly affected by absorption from the continuum. This becomes even more of a concern when imaging data are interpreted. When integrating over the filter bandpass, the emission part of the profile is partly compensated by the absorption. As a result, we measure significantly lower Ly α fluxes than with spectroscopic methods, and the escape fraction of Ly α photons is significantly underestimated. Finally it must be kept in mind that in absence of any prior spectroscopic information on the continuum distribution, the required continuum subtraction could be completely erroneous.

The Ly α line is a premier star-formation tracer, in particular at high z where traditional methods, such as H α or the far-IR emission, become impractical. Radiative transfer effects in the surrounding interstellar gas make its interpretation in terms of star-formation rates less straightforward than often assumed. Clearly, a better understanding of the complex Ly α escape mechanisms, both empirically and theoretically, is required before we can attempt to interpret large-scale Ly α surveys.

A.R.P. acknowledges the hospitality of the Space Telescope Science Institute during his stay as visiting scientist supported by the Director's Discretionary Research Fund. This work was supported by HST grant GO-9470.01-A from the Space Telescope Science Institute, which is operated by the Association of Universities for Research in Astronomy, Inc., under NASA contract NAS5-26555. JMMH has been partially supported by Spanish grant AYA2001-3939-C03-02. GÖ acknowledges support from the Swedish research council and the Swedish national space board.

REFERENCES

- Bergvall, N., Masegosa, J., Östlin, G., & Cernicharo, J. 2000, *A&A*, 359, 41
- Bergvall, N., & Östlin, G. 2002, *A&A*, 390, 891
- Bromm, V., Coppi, P. S., & Larson, R. 2001, *ApJ*, 564, 23
- Charlot, S., & Fall, S. M. 1993, *ApJ*, 415, 580
- Dale, D. A., Helou, G., Neugebauer, G., Soifer, B. T., Frayer, D. T., & Condon, J. J. 2001, *AJ*, 122, 1736
- Frye, B., Broadhurst, T., & Benítez, N. 2002, *ApJ*, 568, 558
- Fujita, S. S., et al. 2003, *AJ*, 125, 13
- Fynbo, J. U., Möller, P., & Thomsen, B. 2001, *A&A*, 374, 443
- Haiman, Z., & Spaans, M. 1999, *ApJ*, 518, 138
- Heisler, C. A., & Vader, J. P. 1995, *AJ*, 110, 87
- Hu, E. M., Cowie, L. L., & McMahon, R. G. 1998, *ApJ*, 502, L99
- Giavalisco, M., Koratkar, A., & Calzetti, D. 1996, *ApJ*, 466, 831

- Kunth, D., Mas-Hesse, J. M., Terlevich, E., Terlevich, R., Lequeux, J., & Fall, S. M. 1998, *A&A*, 334, 11
- Leitherer, C., et al. 1999, *ApJS*, 123, 3
- Malhotra, S., & Rhoads, J. E. 2002, *ApJ*, 565, L71
- Malkan M.A., Gorjian, V., & Tam, R. 1998, *ApJS* 117, 25
- Mas-Hesse, J.M., Kunth, D., Tenorio-Tagle, G., Leitherer, C., Terlevich, R.J., & Terlevich, E. 2003, *ApJ*, submitted
- Melnick, J., Heydari-Malayeri, M., & Leisy, P. 1992, *A&A*, 253, 16
- Neufeld, D. A. 1991, *ApJ*, 370, L85
- Östlin, G. 2000, in *ASP Conf. Ser. 211: Massive Stellar Clusters*, ed. A. Lançon & C. Boily (San Francisco: ASP), 63
- Östlin, G., Amram, P., Bergvall, N., Masegosa, J., Boulesteix, J., & Márquez, I. 2001, *A&A*, 374, 800
- Östlin, G., Amram, P., , Masegosa, J., Bergvall, N., & Boulesteix, J., 1999, *A&AS*, 137, 419
- Östlin, G., Kunth D., 2001, *A&A*, 371, 429
- Ouchi, M. et al. 2003, *ApJ*, 582, 60
- Papaderos, P., Izotov, Y. I., Fricke, K. J., Thuan, T. X., & Guseva, N. G. 1998, *A&A*, 338, 43
- Pavlovsky, C., et al. 2002, *ACS Instrument Handbook, Version 3.0*, Baltimore: STScI
- Partridge, R. B., & Peebles, P. J. E. 1967, *ApJ*, 147, 868
- Pritchett, C. J. 1994, *PASP*, 106, 1052
- Schaerer, D. 2003, *A&A*, 397, 527
- Tenorio-Tagle, G., Silich, S. A., Kunth, D., Terlevich, E., & Terlevich, R. 1999, *MNRAS*, 309, 332
- Thuan, T. X., & Izotov, Y. I. 1997, *ApJ*, 489, 623
- Thuan, T. X., Izotov, Y. I., & Lipovetsky, V. A. 1997, *ApJ*, 477, 661

Vader, J. P., Frogel, J. A., Terndrup, D. M., & Heisler, C. A. 1993, *AJ*, 106, 1743

Vanzi, L., Hunt, L. K., Thuan, T. X., & Izotov, Y. I. 2000, *A&A*, 363, 493

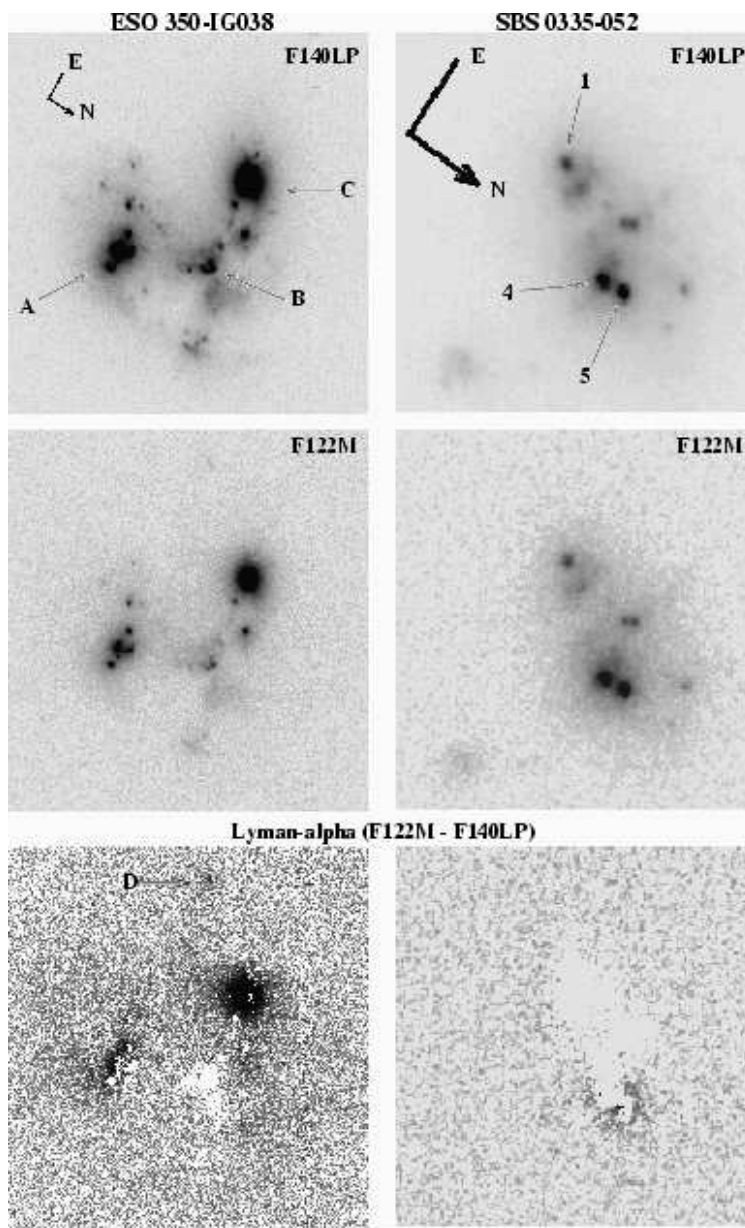


Fig. 1.— HST/ACS images (logarithmic intensity scaling). Top left: UV continuum (F140LP) image for ESO 350-IG038 with the orientation indicated in the upper left corner. The field shown is $13'' \times 13''$. The three main emission regions discussed in the text are labeled A, B and C. Middle left: F122M image of ESO 350-IG038. Lower left: continuum subtracted Ly α image using a relative scaling of 10.3 between F140LP and F122M. Note the faint Ly α emitting blob (labeled D) which is not seen in the continuum image. Top right: UV continuum (F140LP) image for SBS 0335-052. The field shown is $4.4'' \times 4.4''$. The star forming regions discussed in the text are labeled '1', '4' and '5'. Middle right: F122M image of SBS 0335-052. Lower right : continuum subtracted Ly α image. Note the faint emission to the north of '4' and '5'.

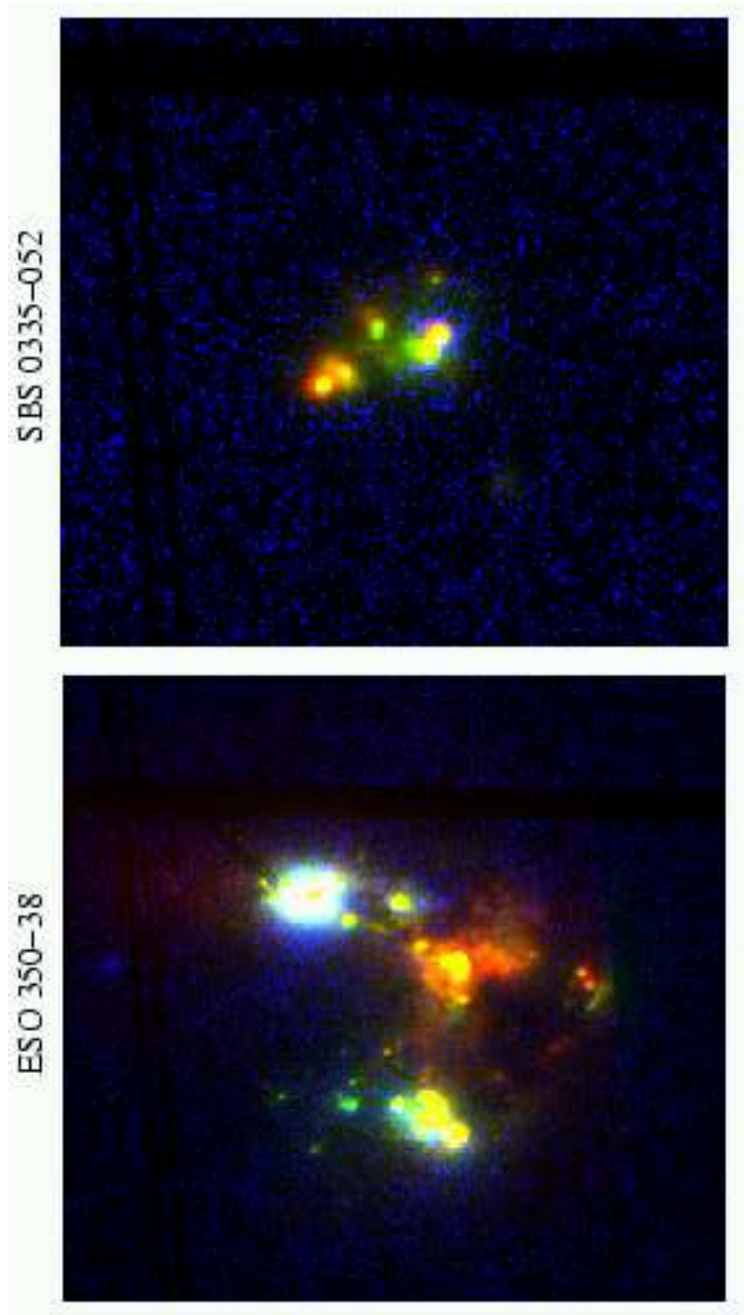


Fig. 2.— Color composite images of the two galaxies, with the optical image coded in red, the F140LP in green and the continuum subtracted Ly α in blue. The spatial scales have been chosen such that both images correspond to the same physical size ($2.3 \text{ kpc} \times 2.3 \text{ kpc}$ for $H_0 = 75 \text{ km s}^{-1} \text{ Mpc}^{-1}$). Left: ESO 350-38, with WFPC2/F606W in the red channel. The size is $13'' \times 13''$. Right: SBS 0335-052, with WFPC2/F791W (taken from the HST archive) in the red channel. The size is $8.3'' \times 8.3''$.